 doi:10.20944/preprints202205.0209.v1

Article

Spatiotemporal Modeling of Zoonotic Arbovirus Transmission in Northeastern Florida using Sentinel Chicken Surveillance and Earth Observation Data

Lindsay P Campbell [1,*], Robert P Guralnick [2], Bryan V Giordano [1], Mohamed F Sallam [3], Amely M Bauer [1], Yasmin Tavares [1], Julie M Allen [3], Caroline Efstathion [4], Suzanne Bartlett [5], Randy Wishard [6], Rui-De Xiu [7], Benjamin Allen [6], Miranda Tressler [5], Whitney Qualls [7], Nathan D Burkett-Cadena [1]

[1] Florida Medical Entomology Laboratory, Department of Entomology & Nematology, IFAS, University of Florida; 200 9th St SE, Vero Beach, FL, 32962, USA; lcampbell2@ufl.edu, nburkettcadena@ufl.edu; b.giordano@ufl.edu
[2] Department of Natural History, Florida Museum of Natural History, University of Florida; Dickinson Hall, University of Florida, Gainesville, FL 32611, USA; rguralnick@flmnh.ufl.edu
[3] Department of Biology, University of Nevada, Reno; 1664 N. Virginia Ave. Reno, NV 89557, USA; msallam@unr.edu, jallen23@unr.edu
[4] Vector Disease Control International; 1320 Brookwood Drive, Suite H, Little Rock, AR 72202, USA; caroline.efstathion@rentokil.com
[5] Volusia County Mosquito Control; 801 South Street, New Smyrna Beach, FL 32168, USA; sbartlettpear@gmail.com, mtressler@volusia.org
[6] City of Jacksonville, Jacksonville Mosquito Control, Jacksonville, Florida 32218, USA; RWishard@coj.net, BenjaminA@coj.net
[7] Anastasia Mosquito Control; St. Augustine, Florida 32092, USA; xueamcd@gmail.com; wqualls@amcdfl.org

* Correspondence: lcampbell2@ufl.edu; Tel.: 772-226-6666

Abstract

The irregular timing and spatial variation in zoonotic arbovirus spillover from vertebrate hosts to humans and livestock present challenges to predicting their occurrence from year to year and within their broader geographic range, compromising effective prevention and control strategies. The objective of this study was to quantify effects of landscape composition and configuration and dynamic temperature and precipitation values on the 2018 spatiotemporal distribution of eastern equine encephalitis virus (EEEV) (*Togaviridae*, *Alphavirus*) and West Nile virus (WNV) (*Flaviviridae*, *Flavivirus*) sentinel chicken seroconversion in northeastern Florida using Earth Observation (EO) data and a modeling framework that incorporated joint spatial and temporal effects. We investigated environmental effects using Bernoulli generalized linear mixed effects models (GLMMs) including a site level random effect, and then added spatial random effects and spatiotemporal random effects in subsequent runs. Models were executed using integrated nested Laplace approximation (INLA) and a stochastic partial differential equation (SPDE) approach in R-INLA. GLMMs that included a spatiotemporal random effect performed better relative to models that included only spatial random effects and better than non-spatial models. Results indicated strong spatiotemporal structure in seroconversion for both viruses, but EEEV exhibited more punctuated and compact structure at the beginning of the sampling season, while WNV exhibited more gradual and diffuse structure across the study area toward the end of the sampling season. Percentage of cypress/tupelo wetland land cover within 3500 m of coop sites and edge density of forest land cover within 500 m had a strong positive effect on EEEV seroconversion, while the best fitting model for WNV was the intercept only model with spatiotemporal random effects. Lagged temperature and precipitation variables included in our study did not have a strong effect on seroconversion for either virus when

 doi:10.20944/preprints202205.0209.v1

accounting for temporal autocorrelation, demonstrating the utility of capturing this structure to avoid Type I errors. Predictive accuracy on out-of-sample data for EEEV seroconversion demonstrates the potential to develop a temporally dynamic framework to predict arbovirus transmission.

Keywords: spatiotemporal modeling; arbovirus transmission; remote sensing; eastern equine encephalitis virus, West Nile virus

1. Introduction

Zoonotic vector-borne pathogens are a leading cause of morbidity and mortality in humans and animals across the globe [1, 2]. The irregular timing and spatial variation in zoonotic arbovirus spillover from vertebrate host species to humans and livestock present challenges to developing effective prevention and control strategies or to developing a basis for predictive modeling. One key advance that may be particularly valuable for predicting zoonotic arbovirus spillover is connecting dense vector and host monitoring data with the widespread availability of multi-scale remotely sensed (RS) environmental data [3, 4]. However, best use of RS data to make linkages to potential spillover has been challenging given the complexity of modeling the spatiotemporal dynamics of these systems [5]. Advances in ecological statistics capable of capturing spatial and temporal covariance and the computational capacity to fit such models [5] provides new opportunities to investigate environmental correlations with zoonotic arbovirus transmission, with the potential to make effective risk predictions and even forecast risk based on future scenarios.

Despite maturity in the tools needed to understand underlying environmental drivers of spatiotemporal dynamics of zoonotic disease risk, empirical applications are still limited, and modeling frameworks are not fully mature. Here we utilize a robust monitoring dataset from efforts by Florida Mosquito Control Districts or Programs and the Florida Department of Health (FDOH) to investigate spatiotemporal environmental correlations with two zoonotic arboviruses of major human and veterinary health importance in the United States; eastern equine encephalitis virus (EEEV) (Togaviridae, *Alphavirus*) and West Nile virus (WNV) (Flaviviridae, *Flavivirus*) [6]. Each virus is maintained in an enzootic cycle primarily between mosquito vectors and passerine amplifying hosts with occasional epizootic transmission resulting in incidental infections, or spillover events, in humans, equines, and other animals [7, 8]. Although symptoms in humans are relatively rare, implications can be severe. Approximately 5% of persons infected with EEEV develop neuroinvasive disease, which can result in lasting neurological symptoms and has a mortality rate of ~30% (CDC 2019), and approximately 1 in 150 people infected with WNV develop neuroinvasive disease with a mortality rate of approximately 10%. Impacts on unvaccinated equines from EEEV and WNV are also severe in animals that develop neuroinvasive disease with fatality rates of 50-70% [9] and 30-40% [10], respectively. These factors, combined with recent geographic expansion of EEEV in the northeastern U.S. [11], and continued epidemics of WNV in multiple regions, demonstrate the need to use methods that can leverage dynamic Earth Observation (EO) data to quantify and predict transmission across space and time to help inform vector control and public health efforts.

While both EEEV and WNV amplify in mosquito-songbird transmission cycles, the mosquito species that are important for vectors for these viruses differ substantially. The primary enzootic mosquito vector of EEEV is *Culiseta melanura*, which breeds in and around freshwater hardwood swamp environments in the Atlantic and Gulf Coast states and the Great Lakes region, and the principal arthropod bridge vectors for transmission to humans or to horses are *Aedes*, *Coquillettidia*, and *Culex* species [7]. West Nile virus is maintained primarily between *Culex* mosquitoes [8, 12] and passerine birds, with multiple primary vectors that vary in distribution by region, habitat, and season [12]. In Florida,

 doi:10.20944/preprints202205.0209.v1

Culex quinquefasciatus and *Culex nigripalpus* are considered primary vectors of WNV with habitats ranging from irrigated agriculture fields to polluted artificial containers in urban areas [13] and multiple bridge vectors competent to transmit WNV to humans and horses are distributed throughout the state [12].

In Florida, EEEV and WNV can exhibit year-round transmission [14]. Multiple studies have incorporated RS environmental data to investigate landscape correlations with EEEV and WNV in the state, including development of a risk index based on EEEV equine cases and surrounding habitats [15, 16], generation of ecological niche models investigating mosquito vectors and sentinel chicken seroconversion at local to state-wide scales [17, 18], and habitat identification for sentinel chicken placement [19]. In addition, seasonality of EEEV sentinel chicken seroconversion was quantified using wavelet analyses with results indicating annual periodicity in seroconversion across Florida and within northern and north central regions [20]. A study quantifying WNV transmission patterns in humans and sentinel chickens found that increased drought conditions followed by wet conditions was correlated with increased human cases and sentinel chicken seroconversion [21]. More recently, researchers found that precipitation, cooling degree days, and El Niño Southern Oscillation Index values were correlated with monthly EEEV equine case counts in the state using distributed lagged non-linear models [22]. These studies all show that climatic and environmental factors likely impact spillover incidence, but they also point to the challenges of accounting for spatiotemporal structuring and dynamics of both observations and covariates to calculate accurate and precise predictions. More complete understanding of environmental drivers of spillover are likely to require direct incorporation of underlying spatiotemporal structure into modeling frameworks, rather than treating spatial and temporal aspects as fully independent.

In 2018, multiple human and equine cases of EEEV and WNV occurred in northeastern Florida with 1 EEEV human case, 14 WNV human cases, 4 EEEV equine cases, and an EEEV infected emu flock [23]. The objective of this study is to quantify effects of landscape composition and configuration and dynamic temperature and precipitation values on the 2018 spatiotemporal distribution of EEEV and WNV sentinel chicken seroconversion in Duval, St. Johns, and Volusia Counties in northeastern Florida. We use a framework that allows a direct way to model spatial and temporal effects, as well as their interactions, which promises to more fully capture the underlying system dynamics. We expect to find higher EEEV seroconversion at chicken coops surrounded with greater percentages and higher edge densities of cypress/tupelo or forested habitats associated with the known habitat of *Culiseta melanura* mosquitoes. We also expect to find that chicken coops surrounded with greater percentages and higher edge densities of semi-urban landscapes will have a strong positive effect on WNV sentinel chicken seroconversion. With regards to seasonal climate factors, we expect to find positive effects of lagged temperature values on sentinel chicken seroconversion for both viruses. Precipitation patterns may have an even stronger effect given results from previous studies, with a positive effect of lagged precipitation values on EEEV seroconversion, and a positive effect of lagged precipitation values near the date of sampling on WNV seroconversion and a negative effect of cumulative precipitation values at distance lags further from the sampling date [21].

2. Materials and Methods

Duval, St. Johns, and Volusia Counties span the northeastern Atlantic Coast of Florida (Figure 1). Developed land cover is distributed along the coastal areas of each county and in a large area in western Volusia County and across most of Duval County (City of Jacksonville). Rural areas are predominantly forest and wetland land cover, interspersed with pastures and cropland. The region's climate is categorized as humid

Preprints (www.preprints.org) | NOT PEER-REVIEWED | Posted: 16 May 2022 doi:10.20944/preprints202205.0209.v1

subtropical [24]. Average temperatures increase with decreasing latitude, with average annual maximum temperatures in the range of 25°C to 29°C and average annual minimum temperatures in the range of 13°C to 17°C. The majority of annual precipitation occurs during the rainy season, typically from May to October, with annual averages ranging from approximately 1150 mm to 1400 mm [25].

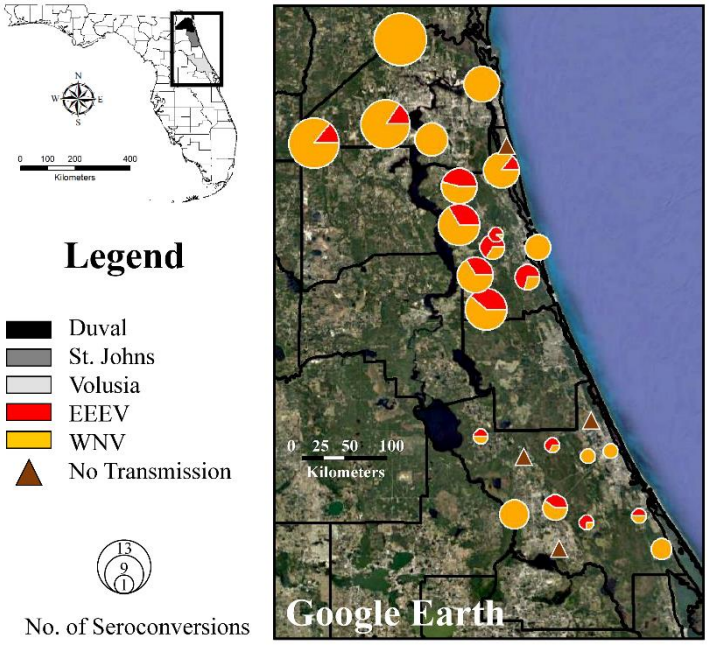

Figure 1. Proportion and abundances of 2018 EEEV and WNV positive seroconverions at sentinel chicken coops across the study area.

Enzootic EEEV and WNV transmission in Florida is detected throughout the early spring to late autumn through an extensive sentinel chicken program, with testing conducted by the Florida Department of Health and participating mosquito control districts across the state, providing site-level and temporally dynamic information about zoonotic pathogen transmission in each area [26, 27]. As part of this effort, dozens of districts in Florida maintain sentinel chicken flocks, which are tested weekly for flavivirus and alphavirus seroconversion, including WNV and EEEV.

Georeferenced 2018 weekly sentinel chicken seroconversion data was cleaned, formatted, and collated across City of Jacksonville Mosquito Control (COJMC) in Duval County, Anastasia Mosquito Control District (AMCD) in St. Johns County, and Volusia Mosquito Control (VMC) districts in northeastern Florida. Data were checked for completeness, including gaps in surveillance across districts and at individual chicken coops. We considered a flock positive for EEEV and a flock positive for WNV if at least one chicken in the flock tested positive for a given week, and we coded the chicken coop as 1 (present) or 0 (absent) for the virus for that week. Sentinel chicken 2018 seroconversion varied across the three counties (Figure 1). The data set included 27 sentinel chicken coop locations, sampled for 28 consecutive weeks between May 1st and November 12th, for a total of 763 observations. A total of 35 sentinel chicken coops tested positive for EEEV and 58 coops tested positive for WNV over the 2018 sampling season.

Preprints (www.preprints.org) | NOT PEER-REVIEWED | Posted: 16 May 2022 doi:10.20944/preprints202205.0209.v1

Land Cover Data

September 2018 Cooperative Land Cover data acquired from the Florida Fish and Wildlife Conservation Commission served as the land cover data for this project [28]. The land cover data set is available at a 10 m spatial resolution. We chose to aggregate classes, given our relatively small study area and limited number of sampling sites because of the large number of fine-scale classes present in the data set and included a total of 11 land cover classes in our analyses (Figure 2).

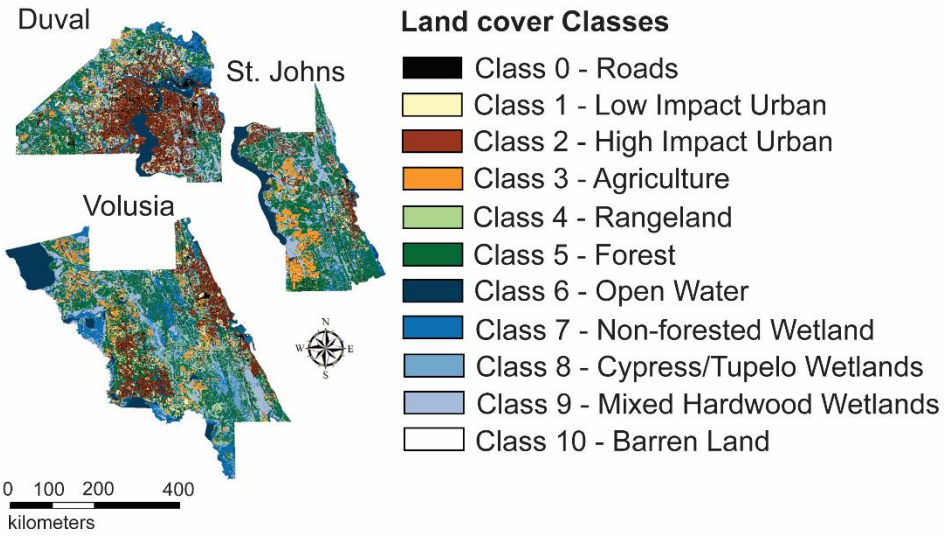

Figure 2. Aggregated land cover classes across each county in the study area.

Landscape metrics quantify the composition and configuration of the landscape or specific land cover type in an area [29]. We chose two landscape metrics for our analyses: percent land cover type for each of our 11 land cover classes within a 500 m, 1000 m, 2000 m, 3500 m, and 5000 m buffer distances from a sentinel chicken site and edge density for multiple land cover classes within these buffer distances from a sentinel chicken site. These metrics define the overall presence of a specific land cover type, while providing information about potential fragmentation, connectivity, or edge habitat in an area [30]. All data were processed using ArcMap v10.6 software program and using the 'landscape metrics' package in R v3.5.1 [31, 32]. Resulting values served as predictor variables in the spatiotemporal GLMM analyses presented below.

Compound topographic wetness index values provide an indication of whether water may pool in a specific geographic area during a precipitation event. Wetness index values are derived from digital elevation models, incorporating the slope of the terrain and a measure of flow direction and accumulation calculated across the study area [33]. We downloaded 30 m resolution ASTER GDEM data from the NASA Earth Data Repository and calculated a compound topographic wetness index using functions available in ArcMap v10.6 software program. Wetness index values were extracted within a 1 km buffer distance of georeferenced sentinel chicken sites, and the mean, maximum, and minimum wetness index values were identified using the 'Zonal Statistics' function in ArcMap.

Climate Data

Preprints (www.preprints.org) | NOT PEER-REVIEWED | Posted: 16 May 2022 doi:10.20944/preprints202205.0209.v1

National Oceanic and Atmospheric Administration (NOAA) NCEP Stage 4 Rainfall 2018 daily data was downloaded for the study area [34]. The data are at a 4 km spatial resolution and were formatted and reprojected to Geographic WGS 84 using the 'Model Builder' application in ArcMap v10.6. Daily precipitation values at georeferenced sentinel chicken sites were extracted before calculating weekly cumulative precipitation values at 9 weekly time lags prior to the sentinel chicken sampling date. Moderate Resolution Imaging Spectroradiometer (MODIS) Terra v6 Land Surface Temperature (LST) 8-day mean composites [35] were downloaded at a 1 km spatial resolution from NASA Earth Data repository (https://earthdata.nasa.gov/). Data were formatted, mosaicked, and reprojected using the MODIS Reprojection Tool, before masking to the study area. Resulting files were filled temporally for missing values, before converting values from Kelvin to Celsius. Land surface temperature values were extracted to georeferenced sentinel chicken sites, and temperature lags (1 - 4 weeks) prior to sentinel chicken sampling served as predictor variables.

Variable Reduction

We performed a conditional random forest executed in the 'caTools' package in R to identify variable importance for EEEV and for WNV seroconversion with the objective of variable reduction prior to generalized linear mixed effects model (GLMM) implementation [36]. Two sets of conditional random forests, one for EEEV and one for WNV, were run with weekly 2018 virus presence/absence serving as the response variable and all landscape metrics at all buffer distances, wetness index values, temperature lags, and precipitation lags serving as the predictor variables. We ranked predictor variables using variable importance values and identified the top six ranking variables for each virus response variable to include in GLMM analyses.

Candidate Sets and Model Runs

We calculated a Pearson's correlation matrix to identify variables that were highly correlated with one another (± 0.6) to construct environmental variable sets for candidate models. We used a Bernoulli generalized linear mixed effects model (GLMM) with a logit link function and individual sentinel chicken coops serving as a site level random effect [37]. Parameters were estimated using maximum likelihood. Covariates were standardized prior to model execution because of varying units across individual variables. Initial models were executed in the 'glmmTMB' package in R [38], and we implemented the 'dredge' function in the MuMIN package to investigate all combinations of variables [39]. We used a model selection approach for evaluation, ranking models from lowest to highest Akaike's Information Criterion (AIC) scores [40], calculated AIC weights, and identified the set of models comprising 95% of the cumulative sum of AIC weights as our confidence set for each virus [41].

Bayesian Modeling

We reran the models comprising the 95% confidence set using integrated nested Laplace approximation (INLA) in the 'INLA' package in R [42] to ensure consistency in parameter estimates with the glmmTMB parameter estimates, and then subsequently

 doi:10.20944/preprints202205.0209.v1

added a spatial random effects term and then spatiotemporal random effects for a total of three sets of models for each virus. INLA is a computationally efficient approach for approximate Bayesian inference, where the posterior marginals of individual parameters (e.g. mean and precision) are approximated, rather than the joint posterior distribution of the model parameters [43, 44]. The spatial random effects were fit using a Gaussian Markov random field using a stochastic partial differential equation (SPDE) approach modeled using a Matérn covariance function [45], and we fit the temporal random effect using a first order autoregressive term (AR1). The SPDE is constructed using constrained Delauney triangulation and we created a convex hull based on sentinel chicken coop locations to define the extent of the triangulation mesh (Supplementary Figure 1). All models were run with default priors, which was a Gaussian prior with mean 0 and precision 0 for the intercept and a Gaussian prior with mean 0 and precision 0.001 for the regression parameters. The SPDE was assigned a multivariate normal prior with mean 0 and penalized complexity priors [46] were estimated for the range and variance with the probability of values being lower than 10,000 for the range set to 0.5 and the probability of the variance being lower than 0.5 set to 0.5.

We ranked models from lowest to highest WAIC and DIC values [47] to identify the best model or set of models, and we observed credible interval values for variables included in top ranking models to determine whether the data supported a predictor variable having a strong effect on EEEV or WNV sentinel chicken seroconversion. A random sample of 30% (n=219) of the seroconversion data was then withheld and the best performing model was rerun with the remaining 70% (n = 534) of the data for out-of-sample prediction. Predictive performance was evaluated by calculating the area under the curve (AUC) of the receiver operating characteristic (ROC) in the 'cutpointr' package in R [48].

An important component in our models was the estimation of Gaussian Markov Random Fields (GMRF) that accounted for spatial and then spatiotemporal structure in our observations [45], and we plotted these values across the study area to provide a visualization for spatiotemporal structure for each week and for each virus during the 2018 sampling season (28 weeks total for each virus). Inclusion of spatial or spatiotemporal terms in the modeling process provides information about the spatiotemporal structure of the observations and can provide clues about environmental variables that may be contributing to an observed process. Additionally, inclusion of these terms can help to reduce Type I errors, owing to residual dependence in space and time between observations in a data set [5, 49].

3. Results

Conditional random forest variable importance values identified a combination of forest and cypress/tupelo wetland land cover and edge densities as top-ranking variables for EEEV, along with weekly cumulative precipitation at a lag of 1 week and 9 weeks. For WNV, the top six variables included a combination of wetland edge density values at multiple buffer distances, and cumulative precipitation values at 1, 3, and 7-week lags. Wetness index values representing the potential for water pooling across the landscape and mean composites of daily temperature values at multiple lag times were not included as candidate variables.

Initial GLMMs using all combinations of candidate model sets using the top 6 variables from the conditional random forest output resulted in 34 models for each virus,

Preprints (www.preprints.org) | NOT PEER-REVIEWED | Posted: 16 May 2022 doi:10.20944/preprints202205.0209.v1

and each virus model set included 8 models that comprised the 95% confidence set based on the sum of the cumulative AIC weights (Supplementary Tables 1 & 2). For EEEV, these 8 models included percent forest within 3500 m and 5000 m, edge density of forest within 500 m, cumulative precipitation lags at 1 and 9 weeks, and percent cypress/tupelo wetlands within 3500 m. For WNV, these 8 models included edge density of wetland within 2000 m, 3500 m, and 5000 m distances and cumulative precipitation at 1, 3, and 7 weekly time lags.

WAIC and DIC results from non-spatial, spatial, and spatiotemporal model runs in the R-INLA environment indicated that all spatiotemporal models performed better than spatial and non-spatial models for EEEV and for WNV (Table 1 & 2). For EEEV, WAIC and DIC scores ranked the spatiotemporal model that included forest edge density within 500 m, cypress/tupelo wetland land cover within 3500 m of sentinel chicken sites, and weekly cumulative precipitation at 9 weeks prior to chicken sampling as the "best" model (Table 5).

Table 1. 95% confidence set of models for EEEV based on the cumulative sum of the WAIC weights. An "X" present in a column cell indicates that the corresponding variable was not included in the model.

Intercept	*3500m percent forest*	*3500 m percent cypress / tupelo wet land*	*500 m edge density forest*	*5000 m percent forest*	*Weekly cumulative precip t-1*	*Weekly cumulative precip t-9*	*DIC*	*WAIC*	*delta WAIC*	*Relative log likelihood*	*WAIC w*	*Sum of the cumulative WAIC w*
-5.465	X	0.755	0.851	X	X	0.139	189.455	178.48	0	1	0.672	0.672
-5.406	X	0.765	0.782	X	0.309	0.168	192.175	180.441	1.961	0.375	0.252	0.924
-5.199	X	0.531	X	0.456	X	0.082	197.896	184.323	5.843	0.054	0.036	0.96

WAIC and DIC scores ranked the spatiotemporal intercept-only model as the "best" model for WNV (Table 2).

Table 2. 95% confidence set of models for WNV based on the cumulative sum of the WAIC weights. An "X" present in a column cell indicates that the corresponding variable was not included in the model.

Intercept	*2000 m edge density wet land*	*Weekly cumulative precip t-1*	*Weekly cumulative precip t-3*	*3500 edge density wet land*	*5000 edge density wet land*	*Weekly cumulative precip t-7*	*DIC*	*WAIC*	*delta WAIC*	*rel LL*	*WAIC w*	*Sum*

Preprints (www.preprints.org) | NOT PEER-REVIEWED | Posted: 16 May 2022 doi:10.20944/preprints202205.0209.v1

-3.687	X	X	X	X	X	X	303.483	298.005	0	1	0.740	0.740
-3.721	X	0.001	-0.110	X	X	X	308.149	302.301	4.296	0.117	0.086	0.827
-3.710	-0.128	-0.005	-0.120	X	X	X	309.626	304.053	6.048	0.049	0.036	0.863
-3.717	X	-0.002	-0.120	-0.100	X	X	309.840	304.188	6.182	0.045	0.034	0.896
-3.717	X	-0.002	-0.120	X	-0.100	X	309.840	304.188	6.182	0.045	0.034	0.930
-3.717	X	0.011	-0.100	X	X	0.088	310.417	304.342	6.336	0.042	0.031	0.961

Credible intervals designated between 0.025 and 0.975 indicate that there is a 95% probability that the parameter estimate is within the interval [44]. Credible intervals for variables included in models in the EEEV 95% confidence set indicated that forest edge density within 500 m of sentinel chicken sites, percent forest within 5000 m, and percent cypress/tupelo wetland coverage within 3500 m had a positive effect on EEEV seroconversion in the study area (Table 3 & Figure 3). Credible intervals indicated that precipitation at lag periods of 1 and 9 weeks did not have a strong effect on EEEV seroconversion, when accounting for spatiotemporal structure, despite these variables being contained within the 95% confidence sets of the non-spatial and spatial model runs (Supplementary Table 3). Results for non-spatial, spatial, and spatiotemporal EEEV INLA models are available in the Supplementary Table 3. Best model results including credible intervals for random effects are available in Supplementary Table 4, and density curves for regression parameters and random effects are available in Supplementary Figure 2.

Table 3. Credible intervals for EEEV 95% confidence set (Model Ranks 1 -3). Variables in bold indicate the data support a strong effect on EEEV seroconversion. The sign of the mean indicates positive or negative effect If values cross zero between the 0.025 quant and the 0.975 quant, the variable is not important to seroconversion.

Model Rank: 1 (best)			
	mean	0.025 quant	0.975 quant
Intercept	-5.4651	-9.5433	-1.3903
Weekly cumulative precip t - 9	0.1386	-0.6905	0.9670
3500 m percent cypress / tupelo wetland	**0.7552**	**0.3056**	**1.2045**
500 m edge density forest	**0.8507**	**0.2203**	**1.4806**

Model Rank 2

Preprints (www.preprints.org) | NOT PEER-REVIEWED | Posted: 16 May 2022 doi:10.20944/preprints202205.0209.v1

	mean	0.025 quant	0.975 quant
Intercept	-5.406	-8.958	-1.856
Weekly cumulative precip t - 9	0.168	-0.662	0.999
500 m edge density forest	**0.782**	**0.136**	**1.426**
3500 percent cypress / tupelo wetland	**0.765**	**0.299**	**1.231**
Weekly cumulative precip t - 1	0.309	-0.246	0.864

Model Rank 3			
value	mean	0.025 quant	0.975 quant
Intercept	-5.199	-8.257	-2.144
Weekly cumulative precip t - 9	0.082	-0.680	0.843
5000 m percent forest	0.456	-0.141	1.051
3500 m percent cypress /tupelo wetland	**0.531**	**0.005**	**1.057**

Preprints (www.preprints.org) | NOT PEER-REVIEWED | Posted: 16 May 2022 doi:10.20944/preprints202205.0209.v1

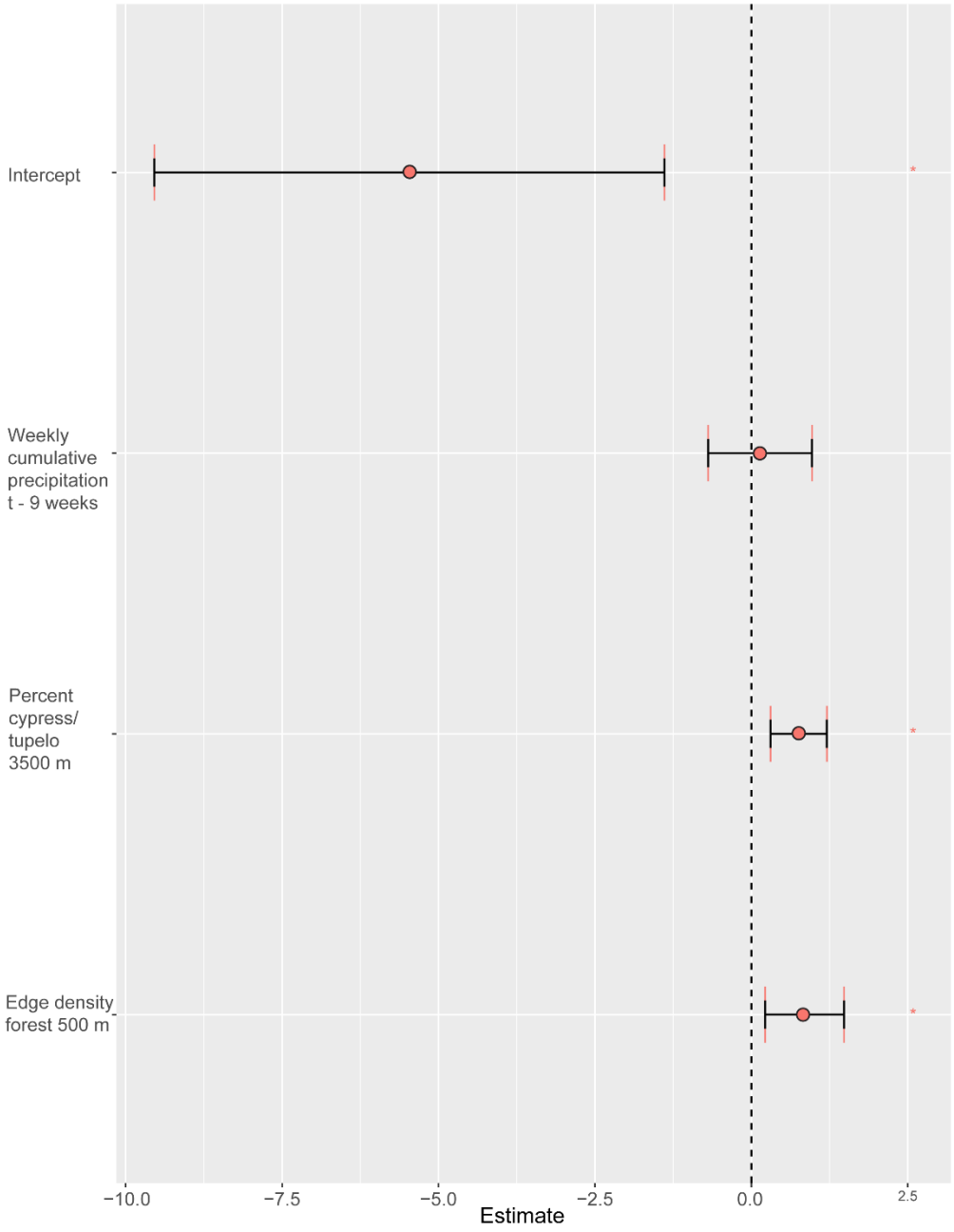

Figure 3. Effect curves of model parameters for environmental variables in the best-fitting EEEV model; credible intervals that do not cross zero indicate a strong positive or negative effect on EEEV seroconversion.

The area under the curve (AUC) of the ROC value for the best EEEV model was 0.948, indicating the potential for accurate prediction (Figure 4). An optimal cutpoint value of 0.157 identified using the 'minimize_metric function' in 'cutpointR' indicated that the model was more accurate at predicting true negative values than true positive values with 2 false negatives and 14 false positives out of 229 records total.

Preprints (www.preprints.org) | NOT PEER-REVIEWED | Posted: 16 May 2022 doi:10.20944/preprints202205.0209.v1

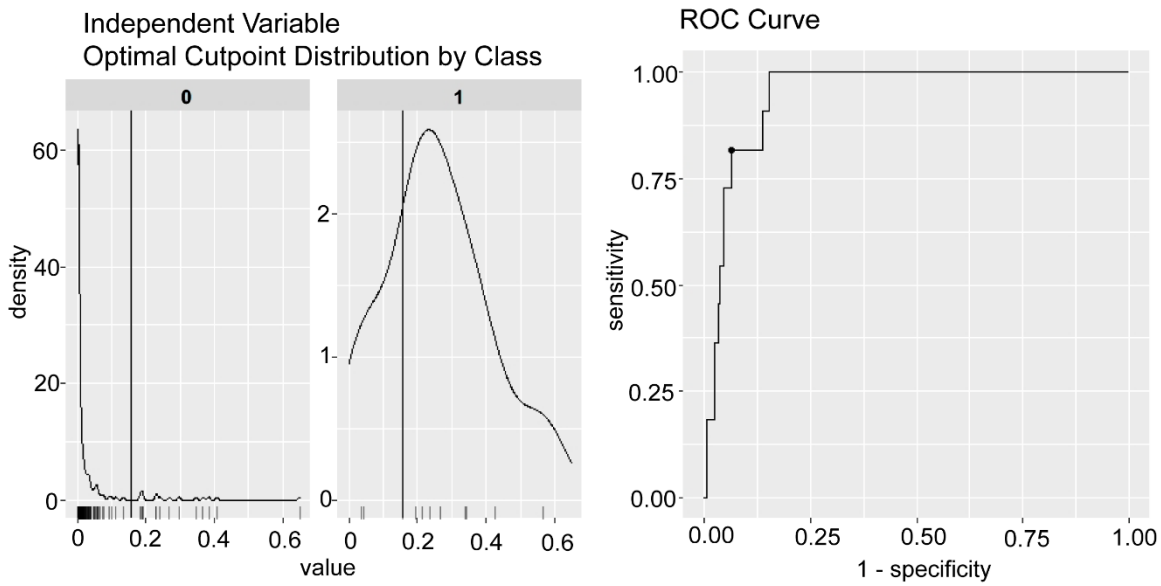

Figure 4. AUC of the ROC for the best EEEV model.

Credible intervals for variables included in the WNV 95% confidence set indicated that none of the variables included in the models had a strong effect on the WNV seroconversion, after accounting for spatiotemporal structure (Table 4). Results for non-spatial, spatial, and spatiotemporal WNV INLA models are available in Supplementary Table 5.

Table 4. Credible intervals for WNV 95% confidence set. No variables had a strong effect on WNV seroconversion. The sign of the mean indicates a positive or negative effect. If values cross zero between the 0.025 quant and the 0.975 quant, the variable has no effect on seroconversion.

Model Rank 1 (best)			
Value	mean	0.025 quant	0.975 quant
Intercept	-3.687	-6.468	-0.909

Model Rank 2			
Value	mean	0.025 quant	0.975 quant
Intercept	-3.721	-6.542	-0.902
Weekly cumulative precip t - 1	0.001	-0.591	0.591
Weekly cumulative precip t - 3	-0.111	-0.670	0.447

Model Rank 3			
	mean	0.025 quant	0.975 quant
Intercept	-3.710	-6.420	-1.002
2000 m edge density wetland	-0.128	-0.476	0.219
Weekly cumulative precip t - 1	-0.005	-0.595	0.585
Weekly cumulative precip t - 3	-0.117	-0.676	0.441

Preprints (www.preprints.org) | NOT PEER-REVIEWED | Posted: 16 May 2022 doi:10.20944/preprints202205.0209.v1

Model Rank 4			
	mean	0.025 quant	0.975 quant
Intercept	-3.717	-6.469	-0.968
3500 m edge density wetland	-0.100	-0.438	0.237
Weekly cumulative precip t - 1	-0.002	-0.593	0.587
Weekly cumulative precip t - 3	-0.115	-0.673	0.444

Model Rank 5			
	mean	0.025 quant	0.975 quant
Intercept	-3.717	-6.469	-0.968
5000 m edge density wetland	-0.100	-0.438	0.237
Weekly cumulative precip t - 1	-0.002	-0.593	0.587
Weekly cumulative precip t - 3	-0.115	-0.673	0.444

Model Rank 6			
	mean	0.025 quant	0.975 quant
Intercept	-3.717	-6.574	-0.862
Weekly cumulative precip t - 1	0.011	-0.587	0.608
Weekly cumulative precip t - 3	-0.101	-0.663	0.460
Weekly cumulative precip t - 7	0.088	-0.376	0.552

Weekly plots of GMRF demonstrated variation in spatiotemporal structure for EEEV and for WNV across the 28-week study period (Figure 5 & 6). Weekly GMRFs for EEEV showed strong spatiotemporal structure at the beginning of the study period, with strongest areas located in St. Johns County and in the southern-central portion of Volusia County (Figure 5). On approximately July 3rd, the spatiotemporal structure began to weaken and dissipate across the remainder of the study period before slight negative spatiotemporal structure developed in the study area.

Preprints (www.preprints.org) | NOT PEER-REVIEWED | Posted: 16 May 2022 doi:10.20944/preprints202205.0209.v1

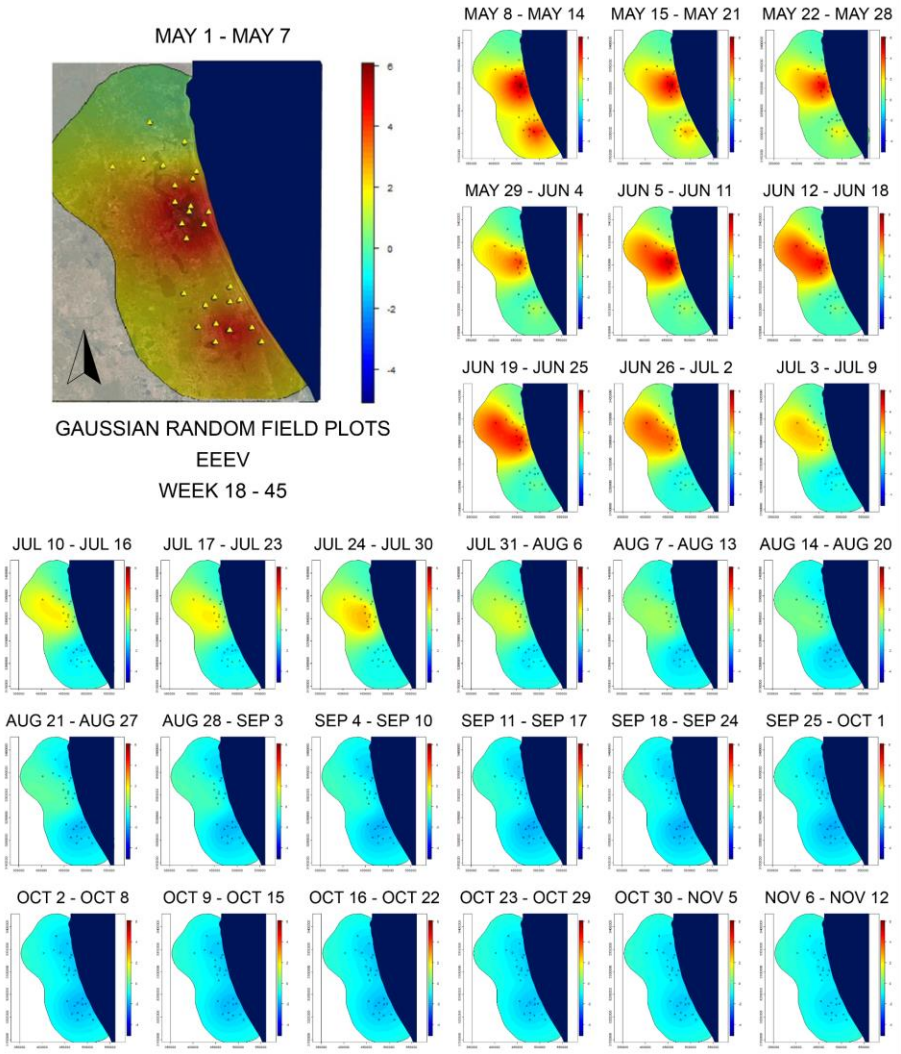

Figure 5. Weekly plots of spatiotemporal Gaussian Markov random fields (GMRF) for weeks 18 - 45 2018 EEEV sentinel chicken seroconversions. A convex hull was generated to create the GMRFs, and GMRFs were clipped to the coastline for visualization. ESRI background imagery was used to map the first plot (May 1 - May 7).

Plots of weekly GMRFs for WNV seroconversion (Figure 6) indicated strong spatiotemporal structure toward the end of the sampling season, moving from a northwest to southeastern direction. Starting ~ July 17th, gradual spatiotemporal structure began in the northwestern corner of the study area building in intensity, and expanding from the northwest in a southwestern direction, before encompassing the entire study area in the week of November 6th.

Preprints (www.preprints.org) | NOT PEER-REVIEWED | Posted: 16 May 2022 doi:10.20944/preprints202205.0209.v1

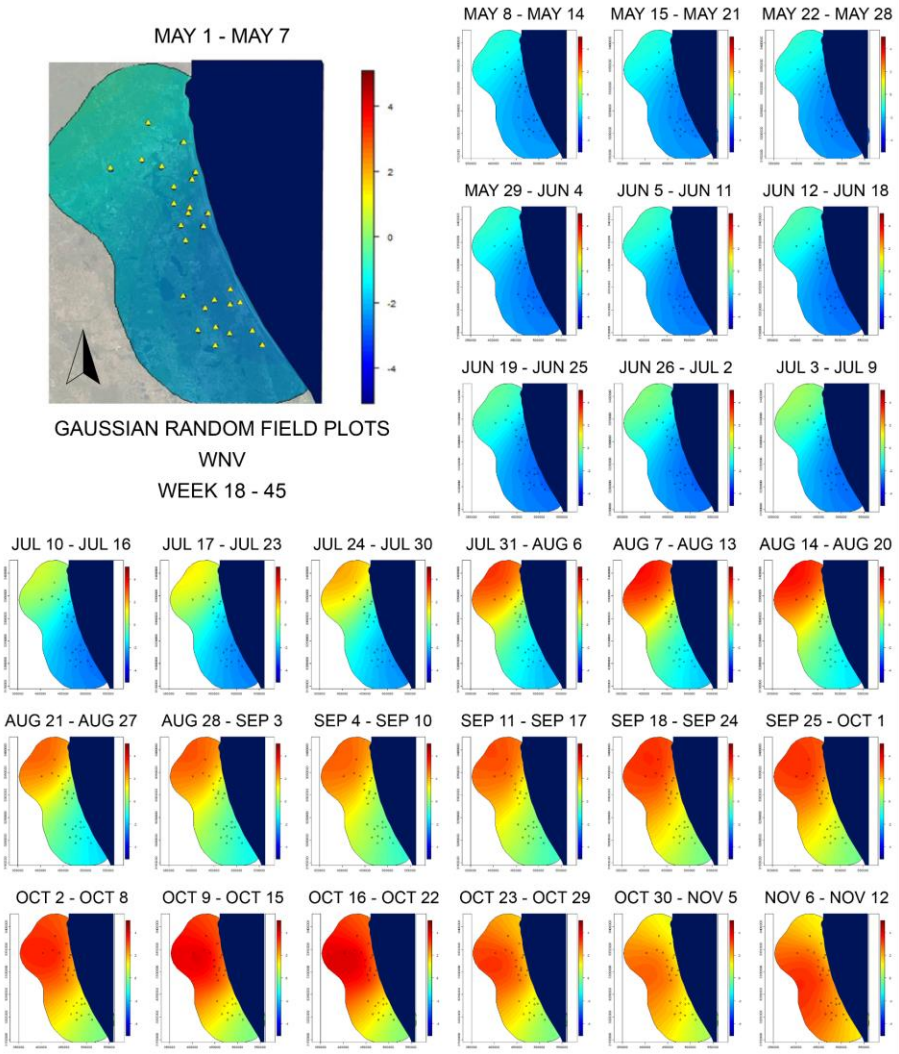

Figure 6. Weekly plots of spatiotemporal Gaussian random fields (GRF) for week 18 - 45 2018 WNV sentinel chicken seroconversions. A convex hull was generated to create the GRFs, and GRFs were clipped to the coastline for visualization. ESRI background imagery was used to map the first plot (May 1 - May 7).

4. Discussion

This study provides new insight into the landscape and climate factors most explanatory of EEEV and WNV sentinel chicken seroconversion in northeastern Florida. In particular, our approach demonstrates the utility of incorporating underlying spatiotemporal structure in model building to improve results. Disease mapping often assumes that disease dynamics remains static across time, even though tools now exist to incorporate spatiotemporal transmission and environmental variables in modeling efforts. Static assumptions are likely unrealistic [50], and the approach we implemented here attempts to account for the joint dependence structure in both space and time. Inclusion of spatiotemporal GMRFs contributed to improved model fits across both virus response variables and demonstrated the need to account for residual spatiotemporal autocorrelation when inferring contributions of environmental variables, in this case cumulative precipitation, to virus ecology.

Model results for EEEV seroconversion were particularly informative, indicating a strong positive effect of cypress/tupelo wetland habitats surrounding chicken coop sites within 3500 m and a strong positive effect of forest edge density within 500 m of coop sites. These results are consistent with the observed breeding habitats of *Cs. melanura* and with previous

 doi:10.20944/preprints202205.0209.v1

investigations of landscape contributions to EEEV. For example, in the northeastern U.S., *Cs. melanura* increased with deciduous or evergreen forested wetlands that had low connectivity to streams and decreased with shrub/scrub wetlands, and higher *Cs. melanura* abundances were strongly associated with higher EEEV infection in mosquito pools [51]. In addition, greater edge density of forest habitat within closer proximities to coop locations suggests that fragmented forest areas may be conducive to dispersal of *Cs. melanura* and/or EEEV bridge vectors, and these results corroborate findings from a previous study in the Florida Panhandle indicating a positive effect of coniferous tree plantations within close proximity to chicken coops on EEEV seroconversion [15].

Strong support for the most parsimonious model ($WAIC_w$ = 0.67), a low number of models comprising the 95% confidence set (n = 3), and the consistent inclusion of cypress/tupelo wetland habitats and forest edge habitats across models indicated that these variables, along with the inclusion of the spatiotemporal GMRFs, have the potential to be predictive of EEEV seroconversion in this area. Results from the ROC analysis reported strong accuracy when predicting presence/absence on out-of-sample data, although closer investigation showed greater accuracy predicting absences than presences. The inclusion of additional sampling data has the potential to improve predictive accuracy, including the ability to predict seroconversion across larger geographic areas and different time periods.

The environmental variables included in our models were less informative for WNV seroconversion than for EEEV. The most parsimonious model was the spatiotemporal intercept only model without covariates, which had strong support ($WAIC_w$ = 0.74), and credible intervals across models included in the 95% confidence set indicated that the data did not support a strong effect of any of the covariates on sentinel chicken seroconversion to WNV. Although we expected to find some correlation with the landscape variables included in our analyses, this result was not altogether surprising given often contradictory results from previous WNV landscape studies in other regions of the U.S. [52, 53]. For example, correlations between WNV and urban and semi-urban environments have been found in multiple U.S. states [17, 54-56] while simultaneously agricultural landscapes have also been indicated [17, 52, 57-60]. Although landscape correlations with WNV are less studied in Florida, the presence of multiple vector species inhabiting a broad range of landscape habitats may be reflected in our model results [12].

To our surprise, the data did not support a strong effect of any of the lagged temperature or precipitation variables included in our analyses, despite the spatiotemporal GMRFs showing clear structure in seroconversion across the study period for each virus and previous studies suggesting the importance of precipitation to observed virus transmission [21, 22]. Although temperature is known to be important to mosquito vector development and can affect virus extrinsic incubation periods [61], the 8-day mean land surface temperature values included in our study were not identified as important variables during the initial variable reduction step for either virus seroconversion. The 9-week lagged cumulative precipitation was included in the 95% confidence set for the non-spatial and spatial EEEV GLMMs, but credible intervals for this variable no longer indicated a strong effect on EEEV seroconversion in the spatiotemporal GLMM, which accounts for temporal autocorrelation. Although not uncommon when working with temporally structured data, this result demonstrates the importance of accounting for residual spatiotemporal autocorrelation to avoid making inferences derived from spurious correlations [49].

Gaussian Markov random field plots provided a visualization of the spatiotemporal structure of EEEV and WNV sentinel chicken seroconversion across the study period and

 doi:10.20944/preprints202205.0209.v1

highlighted differences in patterns between seroconversion of the two viruses. Plots indicated elevated EEEV seroconversion at the very start of the sampling season, with more punctuated and tightly formed structure indicating a smaller effective range compared to the gradual and more diffuse structure of WNV seroconversion at the end of the sampling season. Sampling earlier in the season would likely have captured a more complete distribution of EEEV seroconversion, as well as sampling later in the season for WNV. Climate associations may be stronger towards seasonal onset and offset of infections, arguing for longer sampling periods that can capture those dynamics.

Comparisons of the GMRF plots to FDOH Arbovirus Surveillance Reports of emu, human, and equine cases in the study area [23] suggested potential overlap between active EEEV sentinel chicken seroconversion and the report of an EEEV positive emu flock during the week of May 8 - May 14 in Volusia County in the southernmost region of the study area and also with an equine case during the week of May 25th in St. Johns County (Figure 5). Additional EEEV equine cases occurred in Volusia County during the weeks of June 16th, June 21st, and August 1st. However, these reports did not appear to coincide with active transmission in sentinel chickens in Volusia County during this time period. In addition, a human EEEV case during the week of July 24th in Duval County in the northernmost region of the study area did not appear to coincide with active transmission in sentinel chickens in this area during the week of July 24th, despite activity to the south in St. Johns County. The spatiotemporal GMRF plots for WNV sentinel chicken seroconversion does however suggest potential overlap between the spatiotemporal structure of WNV seroconversion and human cases in the study area. In Duval County (Figure 6), 14 human cases of WNV infection were reported over the study period, with 5 cases reported in August, 3 in September, 4 in October, and 2 in November. Sentinel chicken WNV seroconversion exhibited strong spatiotemporal structure in Duval County beginning in the first week of August and remained relatively strong throughout the remainder of the study period coinciding with the temporal distribution of human cases in the county.

Although we utilized a robust modeling framework, study limitations exist. Specifically, EEEV seroconversion was truncated at the beginning of the sampling season and WNV seroconversion was truncated at the end of the sampling season, preventing the full distribution of transmission events for each virus from being included in the model. Future investigations would benefit from a longer sampling season and the inclusion of additional districts to quantify effects of environmental variables on sentinel chicken seroconversion across broader geographic areas. In addition, the inclusion of spatiotemporal mosquito abundance data in conjunction with environmental variables has the potential to provide important information toward understanding transmission dynamics. Despite these limitations, the use of spatiotemporal modeling frameworks with EO data show significant promise in providing effective means to both map zoonotic arbovirus transmission and understand the environmental drivers (or lack thereof) of transmission risk.

Supplementary Materials:

Supplementary Table 1. Results for EEEV glmmTMB non-spatial models identifying 95% confidence set

Supplementary Table 2. Results for WNV glmmTMB non-spatial models identifying 95% confidence set

Preprints (www.preprints.org) | NOT PEER-REVIEWED | Posted: 16 May 2022 doi:10.20944/preprints202205.0209.v1

Supplementary Table 3. Results for EEEV non-spatial, spatial, and spatiotemporal random effects INLA models (excel file)

Supplementary Table 4. Results for EEEV best model including credible intervals for random effects (excel file)

Supplementary Table 5. Model results for WNV non-spatial, spatial, and spatiotemporal random effects INLA models (excel file)

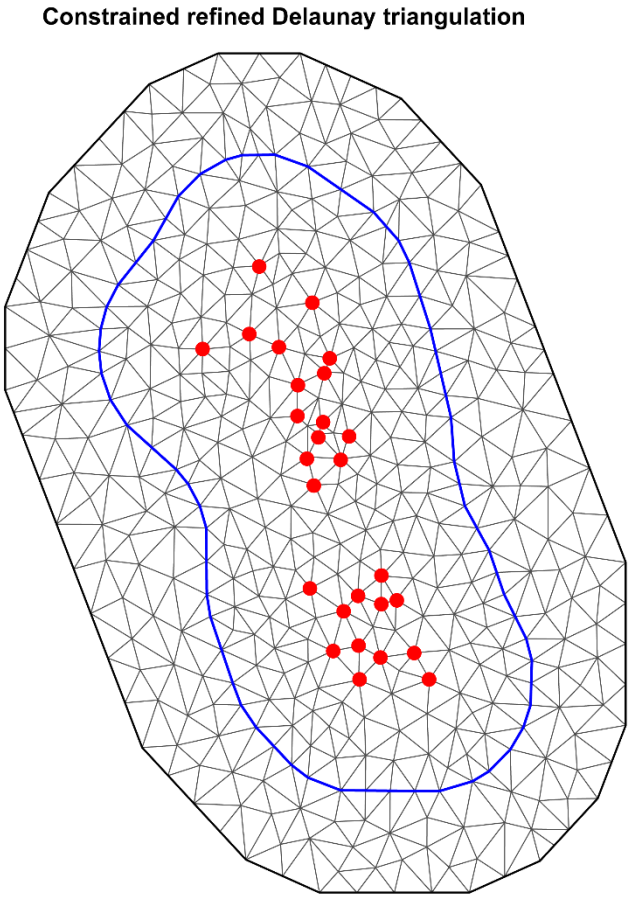

Supplementary Figure 1. Convex hull mesh created for SPDE calculation of spatial covariance matrix.

Preprints (www.preprints.org) | NOT PEER-REVIEWED | Posted: 16 May 2022 doi:10.20944/preprints202205.0209.v1

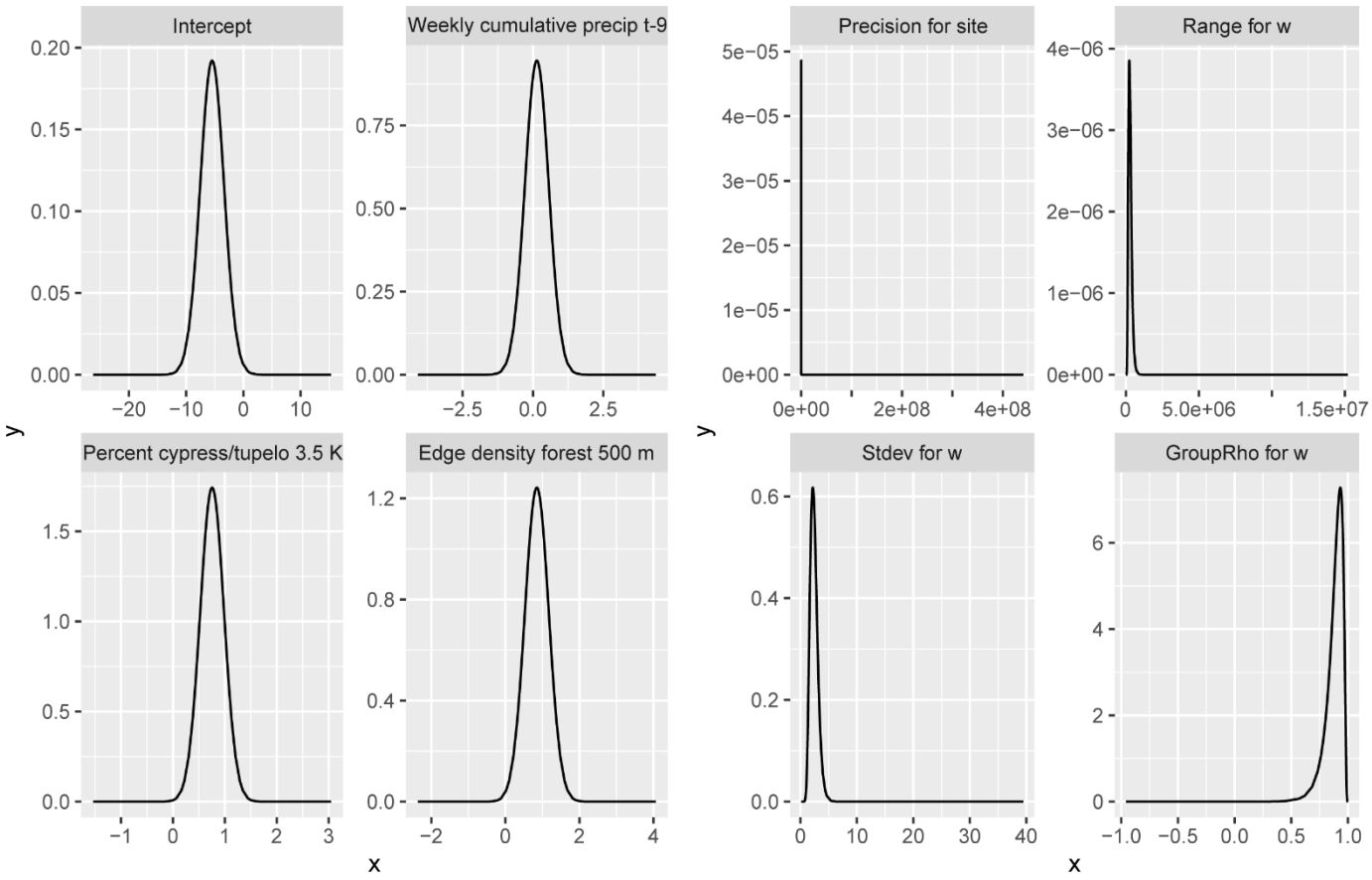

Supplementary Figure 2. Density plots from the best EEEV model for fixed effects and random effects; random effects include the spatial random effects denoted as "Range for w" in the upper right panel and the spatiotemporal random effect denoted as "GroupRho for w"in the lower right panel.

Author Contributions: For research articles with several authors, a short paragraph specifying their individual contributions must be provided. The following statements should be used "Conceptualization, LPC, CE; methodology, LPC, RPG; software, LPC, RPG, BVG; validation, RPG, LPC; formal analysis, LPC and RPG; investigation, LPC, NDBC; resources, SB, RW, RDX; data curation, LPC, BVG, RW, BA, RDX, WQ, SB, MT; writing—original draft preparation, LPC, RPG, MFS, YT, AMB, JMA; writing—review and editing, NDBC, JA, CE, RDQ, WQ, MT, BA, BVG, SB, RW; visualization, BVG, AMB, LPC; supervision, LPC; project administration, LPC; funding acquisition, LPC, NDBC, RDX, RW, SB. All authors have read and agreed to the published version of the manuscript." Please turn to the CRediT taxonomy for the term explanation. Authorship must be limited to those who have contributed substantially to the work reported.

Funding: Please add: This research was funded by the Florida Department of Agriculture and Consumer Services, grant number #026367, the University of Florida Biodiversity Institute Seed Fund, and the USDA National Institute of Food and Agriculture, Hatch project 1021482. Check carefully that the details given are accurate and use the standard spelling of funding agency names at https://search.crossref.org/funding. Any errors may affect your future funding.

Data Availability Statement: In this section, please provide details regarding where data supporting reported results can be found, including links to publicly archived datasets analyzed or generated during the study. Please refer to suggested Data Availability Statements in section "MDPI Research Data Policies" at https://www.mdpi.com/ethics. If the study did not report any data, you might add "Not applicable" here.

Acknowledgments: The authors would like to acknowledge the Florida Department of Health Arbovirus Surveillance Laboratory for conducting sentinel chicken seroconversion testing, mosquito control district personnel, and EE Peterson for comments on the methods section of the manuscript.

 doi:10.20944/preprints202205.0209.v1

Conflicts of Interest: The authors declare no conflict of interest.

References

1. World Health Organization. World health statistics. World Health Organization Report, Geneva, Switzerland. 2013.
2. World Health Organization. Manual on environmental management for mosquito control, with special emphasis on malaria vectors. World Health Organization 1982.
3. Kalluri, S.; Gilruth, P.; Rogers, D.; Szczur, M. Surveillance of Arthropod Vector-Borne Infectious Diseases Using Remote Sensing Techniques: A Review. PLoS Pathog 2007, 3(10), e116.
4. Kitron, U. Landscape Ecology and Epidemiology of Vector-Borne Diseases: Tools for Spatial Analysis. J Med Entomol 1998, 35(4), 435–45.
5. Banerjee, S.; Carlin, B.P.; Gelfand, A.E. Hierarchical modeling and analysis for spatial data. Chapman & Hall/CRC, Boca Raton, Fla. 2004.
6. Lindsey, N.P.; Lehman, J.A.; Staples, J.E.; Fisher, M. West Nile virus and other nationally notifiable arboviral diseases–United States. MMWR Morb Mortal Wkly Rep 2014, 64, 929–34.
7. Scott, T.W.; Weaver, S.C. Eastern Equine Encephalomyelitis Virus: Epidemiology and Evolution of Mosquito Transmission. In: Advances in Virus Research. Maramorosch K, Murphy FA, Shatkin AJ, eds.. Academic Press, 1989. pp. 277-328.
8. Reisen, W.K. Ecology of West Nile virus in North America. Viruses 2013, 5(9), 2079–105.
9. Wisely, S.W.; Hood, K. Fact Sheet: Eastern Equine Encephalitis. Electronic Data Information Source. University of Florida DOI: doiorg/1032473/edis-uw453-2019. 2019.
10. American Association Equine Practitioners. Infectious Disease Guidelines: West Nile Virus [Fact Sheet]. 2017.
11. Armstrong, P.M.; Andreadis, T.G. Ecology and Epidemiology of Eastern Equine Encephalitis Virus in the Northeastern United States: An Historical Perspective. J Med Entomol 2022, 59(1), 1–13,
12. Rochlin, I.; Faraji, A.; Healy, K.; Andreadis, T.G. West Nile Virus Mosquito Vectors in North America. J Med Entomol 2019, 56, 1475-90.
13. Day, J.F.; Tabachnick, W.J.; Smartt, C.T. Factors That Influence the Transmission of West Nile Virus in Florida. J Med Entomol 2015, 52, 743-54.
14. Day, J.F.; Shaman, J. Mosquito-borne arboviral surveillance and the prediction of disease outbreaks. In: Flavivirus encephalitis. Ruzek D, Ed. InTech: Rijeka, Croatia. 2011 pp 105– 130.
15. Vander Kelen, P.T.; Downs, J.A.; Stark, L.M.; Loraamm, R.W.; Anderson, J.H.; Unnasch TR. Spatial epidemiology of eastern equine encephalitis in Florida. Int J Health Geogr 2012, 11(1), 47. doi: 10.1186/1476-072X-11-47.
16. Vander Kelen, P.; Downs, J.; Unnasch, T.; Stark, L. A risk index model for predicting eastern equine encephalitis virus transmission to horses in Florida. Appl Geogr 2014, 48, 79-86.
17. Sallam, M.F.; Xue, R-D.; Pereira, R.M.; Koehler, P.G. Ecological niche modeling of mosquito vectors of West Nile virus in St. John's County, Florida, USA. Parasite Vector 2016, 9, 371. doi: 10.1186/s13071-016-1646-7.
18. Burch, C.; Loraamm, R.; Unnasch, T.; Downs, J. Utilizing ecological niche modelling to predict habitat suitability of eastern equine encephalitis in Florida. Ann GIS. 2020 26(2), 133-47.
19. Beeman, S.P.; Downs, J.A.; Unasch, T.R.; Unnasch, R.S. West Nile Virus and Eastern Equine Encephalitis Virus High Probability Habitat Identification for the Selection of Sentinel Chicken Surveillance Sites in Florida. J Am Mosquito Contr Assoc 2022, 38(1), 1-6.
20. Heberlein-Larson, L.A.; Tan, Y.; Stark, L.M.; Cannons, A.C.; Shilts, M.H.; Unnasch, T.R.; Das, S.R. Complex Epidemiological Dynamics of Eastern Equine Encephalitis Virus in Florida. Am J Trop Med Hyg 2019, 100(5), 1266-74. doi: 10.4269/ajtmh.18-0783.
21. Shaman, J.; Day, J.F.; Stieglitz, M. Drought-Induced Amplification and Epidemic Transmission of West Nile Virus in Southern Florida. J Med Entomol 2005, 42(2), 134-41. doi: 10.1093/jmedent/42.2.134
22. Miley, K.M.; Downs, J.; Beeman, S.P.; Unnasch, T.R. Impact of the Southern Oscillation Index, Temperature, and Precipitation on Eastern Equine Encephalitis Virus Activity in Florida. J Med Entomol 2020, 57(5), 1604-13. doi: 10.1093/jme/tjaa084.
23. Morrison, A.; Giandomenico, D.; Stanek, D.; Heberlein-Larson, L.; Castaneda, M.; Mock, V.; Blackmore, C. Florida Arbovirus Surveillance Week 52: December 23-29 Florida Department of Health. 2018.
24. Kottek, M.; Grieser, J.; Beck, C.; Rudolf, B.; Rubel, F. World Map of the Köppen-Geiger climate classification updated. Meteorol Z, 2006 15(3), 259-63.

25. Winsberg, M.D. Florida weather. 2nd ed University Press of Florida, Gainesville, FL. 2003.
26. Lloyd, A.; Connelly, C.; Carlson, D. Florida Mosquito Control: The state of the mission as defined by mosquito controllers, regulators, and environmental managers. Florida Coordinating Council on Mosquito Control, Vero Beach, FL. 2018.
27. Florida Department of Health (FDOH). Non-Human Mosquito-Borne Disease Monitoring Activities. 2021.
28. Florida Fish and Wildlife Conservation Commission and Florida Natural Areas Inventory. Cooperative Land Cover version 3.5 Raster. Tallahassee, FL. 2021.
29. McGarigal, K.; Marks, B.J. FRAGSTATS: spatial pattern analysis program for quantifying landscape structure. Gen. Tech. Rep. PNW-GTR-351. Portland, OR: U.S. Department of Agriculture, Forest Service, Pacific Northwest Research Station. 1995, p. 122.
30. Gergel, S.E.; Turner, M.G.; Miller, J.R.; Melack, J.M.; Stanley, E.H. Landscape indicators of human impacts to riverine systems. Aquat Sci, 2002, 64(2), 118-28. doi: 10.1007/s00027-002-8060-2.
31. Hesselbarth, M.; Sciaini, M.; With, K.; Wiegand, K.; Nowosad, J. Landscapemetrics: an open-source R tool to calculate landscape metrics. Ecography 2019, 42,1-10.
32. R Core Team. R: A language and environment for statistical computing. R Foundation for Statistical Computing, Vienna, Austria. 2021.
33. Beven, K.J.; Kirkby, M.J. A physically based, variable contributing area model of basin hydrology / Un modèle à base physique de zone d'appel variable de l'hydrologie du bassin versant. Hydrolog Sci J, 1979 24(1), 43-69.
34. Du, J. NCEP/EMC 4KM Gridded Data (GRIB) Stage IV Data. Version 1.0. UCAR/NCAR - Earth Observing Laboratory 2011.
35. Wan, Z.; Zhang, Y.; Zhang, Q.; Zhao-liang, L. Validation of the land-surface temperature products retrieved from Terra Moderate Resolution Imaging Spectroradiometer data. Proc Spie 2002, 83(1), 163–80.
36. Tuszynski, J. caTools: Tools: Moving Window Statistics, GIF, Base 64, ROC AUC, etc. R package version 1.18.0. 2020.
37. Zuur, A.F. Mixed effects models and extensions in ecology with R. Springer, New York, NY. 2009.
38. Brooks, M.E.; Kristensen, K.; van Benthem, K.J.; Magnusson, A.; Berg, C.W.; Nielsen, A.; Skaug, H.J., Machler, M.; Bolker, B.M. glmmTMB Balances Speed and Flexibility Among Packages for Zero-inflated Generalized Linear Mixed Modeling. The R Journal, 2017, 9(2), 378-400.
39. Barton, K. MuMIn: Multi-Model Inference. R package version 1.43.15. 2019.
40. Akaike, H. Information theory and an extension of the maximum likelihood principle", in Petrov, B.N.; Csáki, F., 2nd International Symposium on Information Theory, Tsahkadsor, Armenia, USSR, September 2-8, 1971, Budapest: Akadémiai Kiadó. 1973, 267-81.
41. Burnham, K.P.; Anderson, D.R. Model Selection and Multimodel Inference: A Practical Information-Theoretic Approach (2nd ed.). Springer-Verlag, ISBN 0-387-95364-7. 2002.
42. Lindgren, F.; Rue, H. Bayesian Spatial Modelling with R-INLA. Journal of Statistical Software. 2015, 63(19), 1-25.
43. Rue, R.; Martino, S.; Chopin, N. Approximate Bayesian inference for latent Gaussian models using inte-grated nested Laplace approximations (with discussion). J R Stat B Soc. 2009, 71(2), 319-92.
44. Zuur, A.F.; Ieno, E.N. AA S. Beginner's guide to spatial, temporal, and spatial-temporal ecological data analysis with R-INLA, vol 7. Highland Statistics Ltd, Newburgh. 2017.
45. Lindgren, F.; Rue, H.; Lindstrom, J. An explicit link between Gaussian fields and Gaussian Markov random fields: the stochastic partial differential equation approach. J Roy Stat Soc B 2011, 73(4), 423–98.
46. Simpson, J.E.; Schweinfest, C.W.; Shull, G.E.; Gawenis, L.R.; Walker, N.M.; Boyle, K.T.; Soleimani, M.; Clarke, L.L. PAT-1 (Slc26a6) is the predominant apical membrane Cl-/HCO3- exchanger in the upper villous epithelium of the murine duodenum. Am J Physiol-Gastr L 2007, 292(4), G1079-88.
47. Spiegelhalter, D.J.; Best, N.G.; Carlin, B.R.; Van Der Linde, A. Bayesian measures of model complexity and fit. J Roy Stat Soc B 2002, 64, 583–616.
48. Thiele, C.; Hershfield, G. cutpointr: Improved Estimation and Validation of Optimal Cutpoints in R. J Stat Softw. 2021 98(11), 1-27.
49. Hoeting, J.A. The importance of accounting for spatial and temporal correlation in analyses of ecological data. Ecol Appl 2009, 19, 574–7.
50. Martínez-Beneito, M.A.; López-Quilez, A.; Botella-Rocamora, P. An autoregressive approach to spatio-temporal disease mapping. Stat Med 2008, 27, 2874–89.

 doi:10.20944/preprints202205.0209.v1

51. Skaff, N.K.; Armstrong, P.M.; Andreadis, T.G.; Cheruvelil, K.S. Wetland characteristics linked to broad-scale patterns in Culiseta melanura abundance and eastern equine encephalitis virus infection. Parasite Vector 2017, 10(1), 501.
52. DeGroote, J.P.; Sugumaran, R.; Brend, S.M.; Tucker, B.J.; Bartholomay, L.C. Landscape, demographic, entomological, and climatic associations with human disease incidence of West Nile virus in the state of Iowa, USA. Int J Health Geogr 2008, 7, 19.
53. Bowden, S.E.; Magori, K.; Drake, J.M. Regional differences in the association between land cover and West Nile virus disease incidence in humans in the United States. Am J Trop Med Hyg 2011, 84(2), 234–8.
54. Ruiz, M.O.; Walker, E.D.; Foster, E.S.; Haramis, L.D.; Kitron, U.D. Association of West Nile virus illness and urban landscapes in Chicago and Detroit. Int J Health Geogr 2007, 6,10.
55. Reisen, W.K.; Takahashi, R.M.; Carroll, B.D.; Quiring, R. Delinquent Mortgages, Neglected Swimming Pools, and West Nile Virus, California. Emerg Infect Dis 2008, 14(11), 1747-9.
56. Sallam, M.F.; Michaels, S.R.; Riegel, C.; Pereira, R.M.; Zipperer, W.; Lockaby, B.G.; Koehler, P.G. Spatio-Temporal Distribution of Vector-Host Contact (VHC) Ratios and Ecological Niche Modeling of the West Nile Virus Mosquito Vector, Culex quinquefasciatus, in the City of New Orleans, LA, USA. Int J Env Res Pub He 2017, 14(8), 892.
57. Eisen, L.; Barker, C.M.; Moore, C.G.; Pape, W.J; Winters, A.M.; Cheronis, N. Irrigated Agriculture Is an Important Risk Factor for West Nile Virus Disease in the Hyperendemic Larimer-Boulder-Weld Area of North Central Colorado. J Med Entomol 2010, 47(5), 939–51.
58. Crowder, D.W.; Dykstra, E.A.; Brauner, J.M.; Duffy, A.; Reed, C.; Martin, E.; Peterson, W.; Carriere, Y.; Dutilleul, P.; Owen, J.P. West Nile Virus Prevalence across Landscapes Is Mediated by Local Effects of Agriculture on Vector and Host Communities. PLOS ONE 2013, 8(1), e55006.
59. Kovach, T.J.; Kilpatrick, A.M. Increased Human Incidence of West Nile Virus Disease near Rice Fields in California but Not in Southern United States. Am J Trop Med Hyg 2018, 99(1), 222-8.
60. Dunphy, B.M.; Kovach, K.B.; Gehrke, E.J.; Field, E.N.; Rowley, W.A.; Bartholomay, L.C.; Smith, R.C. Long-term surveillance defines spatial and temporal patterns implicating Culex tarsalis as the primary vector of West Nile virus. Sci Rep 2019, 9(1), 6637. doi: 10.1038/s41598-019-43246-y.
61. Mullen, G.R.; Durden, L.A. Medical and Veterinary Entomology. (Third Edition), 2019 Academic Press.